



DGE-seq analysis of *MUR3*-related *Arabidopsis* mutants provides insight into how dysfunctional xyloglucan affects cell elongation

Zongchang Xu^{a,b}, Meng Wang^{a,b}, Dachuan Shi^a, Gongke Zhou^c, Tiantian Niu^a, Michael G. Hahn^{d,e}, Malcolm A. O'Neill^d, Yingzhen Kong^{a,*}

^a Key Laboratory for Tobacco Gene Resources, Tobacco Research Institute, Chinese Academy of Agricultural Sciences, Qingdao 266101, PR China

^b Graduate School of Chinese Academy of Agricultural Science, Beijing 100081, PR China

^c Qingdao Engineering Research Center of Biomass Resources and Environment, Qingdao Institute of Bioenergy and Bioprocess Technology, Chinese Academy of Sciences, Qingdao 266101, PR China

^d Complex Carbohydrate Research Center, University of Georgia, Athens, GA 30602-4712 USA

^e Department of Plant Biology, University of Georgia, Athens, GA 30602-4712 USA

ARTICLE INFO

Article history:

Received 13 July 2016

Received in revised form

14 November 2016

Accepted 14 January 2017

Available online 30 January 2017

Keywords:

Arabidopsis

MUR3

Xyloglucan

Cell elongation

Hypocotyl

DGE-seq

ABSTRACT

Our previous study of the *Arabidopsis mur3-3* mutant and mutant plants in which the *mur3-3* phenotypes are suppressed (*xxt2mur3-3*, *xxt5mur3-3*, *xxt1xxt2mur3-3* and *35Spro:XLT2:mur3-3*) showed that hypocotyl cell elongation is decreased in plants that synthesize galactose-deficient xyloglucan. To obtain genome-wide insight into the transcriptome changes and regulatory networks that may be involved in this decreased elongation, we performed digital gene expression analyses of the etiolated hypocotyls of wild type (WT), *mur3-3* and the four suppressor lines. Numerous differentially expressed genes (DEGs) were detected in comparisons between WT and *mur3-3* (1423), *xxt2mur3-3* and *mur3-3* (675), *xxt5mur3-3* and *mur3-3* (1272), *xxt1xxt2mur3-3* and *mur3-3* (1197) and *35Spro:XLT2:mur3-3* vs *mur3-3* (121). 550 overlapped DEGs were detected among WT vs *mur3-3*, *xxt2mur3-3* vs *mur3-3*, *xxt5mur3-3* vs *mur3-3*, and *xxt1xxt2mur3-3* vs *mur3-3* comparisons. These DEGs include 46 cell wall-related genes, 24 transcription factors, 6 hormone-related genes, 9 protein kinase genes and 9 aquaporin genes. The expression of all of the 550 overlapped genes is restored to near wild-type levels in the four *mur3-3* suppressor lines. qRT-PCR of fifteen of these 550 genes showed that their expression levels are consistent with the digital gene expression data. Overexpression of some of these genes (*XTH4*, *XTH30*, *PME3*, *EXPA11*, *MYB88*, *ROT3*, *AT5G37790*, *WAG2* and *TIP2;3*) that are down-regulated in *mur3-3* partially rescued the short hypocotyl phenotype but not the aerial phenotype of *mur3-3*, indicating that different mechanisms exist between hypocotyl cell elongation and leaf cell elongation.

© 2017 Elsevier B.V. All rights reserved.

1. Introduction

Xyloglucan is a hemicellulosic polysaccharide present in the primary cell walls of all land plants studied to date [1,2]. *Arabidopsis* and numerous other flowering plants synthesize a XXXG-type

xyloglucan [3,4] in which two of the α -D-xylosyl residues (X side chain) attached to the β -glucan backbone are often substituted at O-2 with a β -D-Galp residue (L side chain: XLG, XXLG and XLLG). The Gal residue of the L side chain adjacent to the unsubstituted G is often substituted at O-2 with a α -L-Fucp residue (F side chain: XXFG and XLFG) [4].

The *Arabidopsis* glycosyltransferases (GTs) involved in xyloglucan side chain biosynthesis have been identified [5–10]. These GTs include two XYLOGLUCAN XYLOSYLTRANSFERASES (XXT1 and XXT2) that add xylosyl residues to the glucan backbone [9], XXT5 may also participate in this process but is not essential [10]. XYLOGLUCAN L-SIDE CHAIN GALACTOSYLYLTRANSFERASE2 (XLT2) adds Gal to the middle Xyl (L side chain) [5], whereas MURUS3 (MUR3) adds Gal to the Xyl adjacent to the unbranched Glc (L side chain) [6]. FUCOSYLTRANSFERASE1 (FUT1) adds a Fuc residue to

Abbreviations: DGE-seq, digital gene expression sequencing; WT, wild type; GO, Gene Ontology; DEGs, differentially expressed genes; GTs, glycosyltransferases; RPKM, reads per kilobases per million reads; KEGG, kyoto encyclopedia of genes and genomes; TFs, transcription factors; BR, brassinosteroids; WGCNA, weighted gene co-expression network analysis.

* Corresponding author.

E-mail addresses: xuzc1110@163.com (Z. Xu), menglihua@yeah.net (M. Wang), shidc@qibebt.ac.cn (D. Shi), zhougk@qibebt.ac.cn (G. Zhou), tian1528861055@163.com (T. Niu), hahn@ccrc.uga.edu (M.G. Hahn), mao@ccrc.uga.edu (M.A. O'Neill), kongyingzhen@caas.cn (Y. Kong).

the MUR3Gal (F side chain) [7]. The XLFG, XXXG and XXFG sub-units account for 43%, 25% and 24%, respectively of *Arabidopsis* xyloglucan [11].

Arabidopsis plants carrying mutations that affect individual GTs have altered xyloglucan structure or content [5,8,12–15]. The amounts of Fuc substitution are reduced by at least 98% in the *fut1* mutant, yet the plants grow normally and the strength of their walls is comparable with wild type (WT) [12]. The XLXG and XLFG sub-units are almost completely absent in the *xlt2* mutant xyloglucan, but there are only subtle phenotypic difference between *xlt2* and WT [5]. In *xxt1*, *xxt2* and *xxt5* mutants the xyloglucan content of the wall is reduced by approximately 10%, 32% and 50%, respectively, compared with WT [8,13]. The *xxt1* and *xxt2* mutants have no visible morphological phenotype [13] whereas *xxt5* forms short root hairs that have bubble-like extrusions at their tip and roots that have altered morphology [15]. Somewhat surprisingly, the *xxt1xxt2* double mutant, which lacks detectable amounts of xyloglucan in its cell wall [13], only exhibits modest phenotypes including short root hairs with bulging bases [13], somewhat shorter hypocotyls and stems, and altered cellulose microfibril organization [14]. The mechanical properties of *xxt1xxt2* cell walls including wall stiffness, creep and stress relaxation also differ from WT [16]. Nevertheless, the *xxt1xxt2* mutant, which is typically a little smaller than its WT, counterpart develops normally [16]. The *mur3* mutants have pleiotropic phenotypes [17]. Plants carrying the S470L (*mur3-1*) or the A290V (*mur3-2*) point mutation in *MUR3* are visibly similar to WT plants [6,18]. However, these mutants are leaky as they synthesize xyloglucan containing discernible amounts of the F side-chain (XXFG and XLFG subunits) [19]. By contrast, *mur3-3* and *mur3-7*, which are T-DNA knock-out lines of *MUR3*, are dwarfed with a cabbage-like growth phenotype, form shorter etiolated hypocotyls, and have a endomembrane aggregation phenotype [17]. The *mur3-3* has also been reported to be hypersensitive to salt stress [20] and constitutively resistant to infection by *Hyaloperonospora parasitica* [21]. The xyloglucan from *mur3-3* plants is composed of XXXG and XLXG subunits and contains no detectable amounts of the F side-chain [19].

Our previous study established that most of the *mur3-3* phenotypes, including short hypocotyls, curled leaf and endomembrane aggregation is rescued by knocking out *XXT2* or *XXT5* individually or by knocking out both *XXT1* and *XXT2* [19]. The *xxt2mur3-3* and *xxt5mur3-3* mutants produce xyloglucan that is still composed of XXXG and XLXG subunits, but the XLXG subunit accounts for 60% and 72% of the xyloglucan subunits, respectively, which is almost double its abundance in *mur3-3* [19]. This result suggests that the *mur3-3* phenotype results from the reduced abundance of the XLXG subunit. This notion is supported by the finding that overexpressing *XLT2* in *mur3-3* (35Spro:*XLT2:mur3-3*) increased the abundance of the XLXG subunit and suppressed the *mur3-3* mutant phenotypes. We also found that the growth of *mur3-3* was restored to near normal by abolishing their ability to synthesize xyloglucan by introducing the *xxt1xxt2* double mutation (*xxt1xxt2mur3-3*).

The lack of a strong phenotype in the *xxt1xxt2* double mutant that forms no discernible amounts of xyloglucan has challenged the hypothesis that the strength and extensibility of the primary cell wall is controlled by a cellulose-xyloglucan load-bearing network [22]. The near normal appearance of this mutant has also led to questions about the role of xyloglucan in plant growth and development. Based on our previous data we proposed that galactose-deficient xyloglucan is dysfunctional and that its presence in the cell wall is more deleterious to cellular processes than the complete absence of xyloglucan.

There is increasing evidence that changes in wall structure are perceived by the cell and then relayed to the cytosol to elicit numerous responses [23]. Several proteins that may sense cell wall changes have been described including the receptor-like kinase

THESEUS [24], and the pectin-binding wall-associated kinases [25]; however, the cellular signaling pathways involved are largely unknown [26]. The *mur3-3* mutant provides a unique opportunity to increase our understanding of how changes in cell wall polysaccharide biosynthesis and structure affect plant growth. However, it is not known how a seemingly small change in the structure of single cell wall polysaccharides can lead to substantial growth defects. To address this question, we performed digital gene expression analysis on the etiolated hypocotyls of WT and *mur3-3* plants as well as four mutant plants (*xxt2mur3-3*, *xxt5mur3-3*, *xxt1xxt2mur3-3* and 35Spro:*XLT2:mur3-3*) in which the *mur3-3* phenotypes are suppressed.

2. Materials and methods

2.1. Plant materials, seeds sterilization and growth conditions

All *Arabidopsis* plants used in this study were in the Columbia (Col-0) background. The homozygous T-DNA insertion mutant lines *mur3-3* (*At2g20370*; Salk_141953), *xxt2mur3-3* (*XXT2*, *At4g02500*; SALK_101308), *xxt5mur3-3* (*XXT5*, *AT1G74380*; GK_411G05), *xxt1xxt2mur3-3* (*XXT1*, *At3g62720*; SAIL_785_E02) and the *XLT2* over-expression line 35Spro:*XLT2:mur3-3* were generated as described previously [19]. Seeds were treated with aq. 10% NaClO for 5 min and then washed three times with sterile water. Sterilized seeds were transferred to ½ strength Murashige and Skoog agar and kept in the dark for 48 h at 4 °C. The seeds were then grown for 5 days at 20 °C in the absence of light. Three replicates of sterilized seeds were prepared for each genotype. Approximately 200 hypocotyls were randomly selected from each of the three replicates and immediately frozen in liquid nitrogen prior to total RNA isolation for DGE sequencing. For hypocotyl length measurement, images of at least ten seedlings of each genotype were obtained using a Canon 5D Mark III digital camera. The length measurement of hypocotyls was performed using ImageJ software [27].

2.2. RNA extraction, preparation of digital expression libraries and Illumina sequencing

Total RNA was extracted with QIAGEN RNeasy® Plant Mini Kit (QIAGEN, Cat. NO. 74903). DNase was used to digest genomic DNA. RNA purity was assessed using a NanoPhotometer® spectrophotometer (IMPLEN, CA, USA). The amounts of RNA were measured using a Qubit® RNA Assay Kit (Life Technologies, CA, USA) and RNA integrity was assessed using a RNA Nano 6000 Assay Kit of the Bioanalyzer 2100 system (Agilent Technologies, CA, USA). A total of 3 µg purified RNA from each plant line was used to generate the Illumina sequencing libraries using a NEBNext® Ultra™ RNA Library Prep Kit for Illumina® (NEB, USA) following the manufacturer's recommendations. The libraries were sequenced using a Illumina Hiseq 2000/2500 platform by Beijing Novogene Bioinformatics Technology Co. Ltd (Beijing, China).

2.3. Analysis of digital gene expression reads and identification of expressed genes

The raw data was filtered to eliminate reads containing adapter, poly-N and low quality reads. The Q20, Q30 and GC content of the cleaned data were then calculated to determine the quality of the reads. The single-end clean reads were then mapped to the *A. thaliana* reference genome using TopHat v2.0.9 [28]. Only reads with a perfect match or at most two bases of mismatch were permitted in the alignment. HTSeq v0.6.1 was used to calculate the number of reads mapped to each gene (read counts data) [29]. Reads Per Kilobases per Million mapped reads (RPKM), which considers

the effect of sequencing depth and gene length for the read counts at the same time and is currently the most commonly used method for estimating gene expression levels in DGE analysis [30], was used to estimate the expression level of each gene. In this study, the expressed gene was defined by RPKM value greater than 1.

2.4. Differential expression analysis

Prior to differential gene expression analysis for each sequenced library, the read counts data were adjusted by the TMM method [31]. Differential expression analysis of two libraries was performed using the DESeq R package (1.12.0) [32]. The P-values, which indicate significant differences of transcript accumulation was adjusted using the Benjamini and Hochberg method [33]. A combination of the corrected P-value <0.005 and the absolute value of $\log_2(\text{fold change}) \geq 1$ were used as the thresholds to assess the significance of differences in gene expression.

2.5. GO, KEGG and MapMan enrichment analysis and gene classification analysis

GO functional categories were assigned to the differentially expressed genes using the web-based agrIGO tools [34]. GO enrichment analysis of DEGs was implemented using singular enrichment analysis (PAGE) by comparing a query list of differentially expressed genes to a background gene set (FDR <0.05 was as criteria). KOBAS software [35] was used for pathway enrichment analyses by testing the statistical enrichment of DEGs in KEGG pathways. MapMan tool [36] was used for overview of metabolic pathways, regulatory processes and biotic stress processes.

2.6. Annotation of TFs and cell wall-related genes

TF family members were annotated based on a published data [37]. Cell wall-related genes were annotated based on the Purdue Cell-Wall-Genomics Database (<http://cellwall.genomics.purdue.edu/>).

2.7. Promoter conserved motifs and WGCNA analysis

72 down-regulated and 30 up-regulated DEGs in *mur3-3* compared with WT and the four suppressor lines were used for promoter conserved motifs analysis. 2 kb length promoters of the 102 overlapped DEGs were analyzed using the web based tool (<http://www.bioinformatics2.wsu.edu/cgi-bin/Athena/cgi/home.pl>). The occurrence of detected conserved motifs was further screened using the P-value result (P-value result <0.05 was as criteria). The weighted gene co-expression network analysis (WGCNA) was performed in R using the WGCNA package, as previously described [38]. Differentially expressed genes including cell wall-related genes, hormone-related genes, TFs, genes encoding the kinase protein, aquaporin and chlorophyll a-b binding protein were used to construct an unsupervised co-expression based similarity matrix using Pearson's correlation coefficient. The R package WGCNA version 1.35 was then used to create the networks [38], which were visualized with Cytoscape 3.2 [39].

2.8. Plant transformation and complementation test

A total of 11 DEGs including cell wall-related genes, TFs, hormone-related genes, kinase genes and an aquaporin gene, which were down-regulated in *mur3-3* compared with WT and the suppressor lines were overexpressed in *mur3-3*. The full-length CDS sequences of each gene were cloned into the *Xba*I and *Kpn*I sites downstream of the cauliflower mosaic virus 35S promoter in the *pCam35tlegfp2#4* vector [19]. The constructs were introduced

into *Agrobacterium* strain GV3101, and the bacteria were used to transform *mur3-3* mutant plants by a floral dip transformation method [40]. Transgenic plants were selected by growth on $\frac{1}{2}$ strength MS medium containing hygromycin (15 mg/L). The presence of the transgene was confirmed by PCR using the gene-specific primer paired with vector-specific primer. The hygromycin resistant T₁ transgenic plants and *mur3-3* seedlings were then grown in controlled-environmental growth chambers at 19 °C with a 16-h-light and 8-h-dark cycle for phenotype observation. Seeds treatment and hypocotyl measurement of T₂ transgenic plants were the same as described in 2.1 above.

2.9. Quantitative RT-PCR

RNA for qRT-PCR analysis was extracted from the hypocotyls of six plants as described above. First-strand cDNA was synthesized from 1 μg of DNA-free RNA using a TransScript® One-Step gDNA Removal and cDNA Synthesis SuperMix Kit (TransGen, AT311-02) according to the manufacturer's instructions. The qRT-PCR mixture (20 μL total volume) contained 10 μL of SYBR Green super mix (Roche Diagnostics GmbH, Mannheim, Germany), 3 μL of each primer (2 μM), 1 μL of cDNA, and 3 μL of RNase-free water. The reactions were performed on an Applied Biosystems 7500 Real-Time PCR system according to the manufacturer's instructions. All reactions were performed in three biological replicates with three technical replicates each. Expression was calculated as $2^{-\Delta\Delta Ct}$ [41] and normalized to that of the *TUBLIN* gene. The primer sets were designed using Primer-BLAST (<http://www.ncbi.nlm.nih.gov/tools/primer-blast/>) to avoid non-specific amplification. Primers used in this study were shown in Supplementary file 1.

3. Results

3.1. DGE library sequencing and mapping sequences to the reference genome

The *mur3-3* mutant has a significantly shorter hypocotyl length than WT. Hypocotyl length is restored to near normal in each of the four suppressor lines (Fig. 1). To investigate

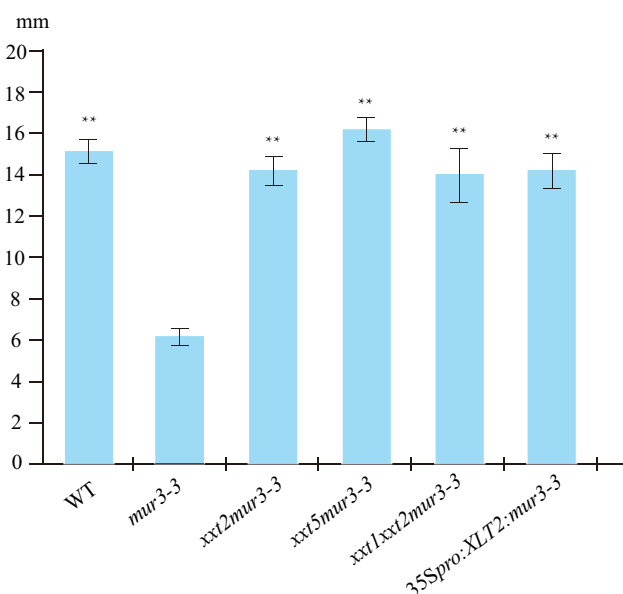


Fig. 1. Etiolated hypocotyl length of WT, *xxt2mur3-3*, *xxt5mur3-3*, *xx1xxt2mur3-3*, *35Spro:XLT2:mur3-3* and *mur3-3*. Hypocotyls from at least ten seedlings of each of the six plant lines were measured. Data shown are average \pm SD. (Student's two-tailed t-test with *mur3-3*; ** $P < 0.01$).

Table 1

Summary of reads numbers based on DGE-seq of the six plant lines and the number of reads mapped to the genome.

Sample name	Wild type	<i>mur3-3</i>	<i>xxt2mur3-3</i>	<i>xxt5mur3-3</i>	<i>xxt1xxt2mur3-3</i>	35Spro: <i>XLT2:mur3-3</i>
Raw reads	15225291	10980105	16935349	11712348	10403746	12378356
Clean reads	14789989	10793421	16686602	11551898	10225651	12207798
Clean ratio	97.14%	98.30%	98.53%	98.63%	98.29%	98.62%
clean bases (Mb)	740	540	830	580	510	610
Q20 (%)	99.04	98.96	99.03	98.95	99.03	98.84
GC content (%)	45.26	45.92	45.48	45.31	45.65	45.48
Total mapped reads	14350871	10446763	16213637	11172751	9887405	11790956
Mapping ratio	97.03%	96.79%	97.17%	96.72%	96.69%	96.59%

the gene expression patterns in these six plant lines, RNA was extracted from the hypocotyls and sequenced using the Illumina Hiseq 2000/2500 platform. After the removal of adaptor sequences, duplicate sequences, ambiguous reads and low-quality reads we obtained broadly similar numbers of cleaned reads from WT (14789989), *mur3-3* (10793421), *xxt2mur3-3* (16686602), *xxt5mur3-3* (11551898), *xxt1xxt2mur3-3* (10225651), and 35Spro:*XLT2:mur3-3* (12207798) (Table 1). The average percentage ratio of clean reads was 98.25% among the six libraries. The average Q20 percentage of the six libraries was 98.98% and the average GC was 45.52% (Table 1). Saturation and mean coverage analysis results showed that the DGE-seq data reads were distributed uniformly over the transcript and that their quality was suitable for quantitative expression analysis (Fig. S1).

The cleaned reads from WT (14350871), *mur3-3* (10446763), *xxt2mur3-3* (16213637), *xxt5mur3-3* (11172751), *xxt1xxt2mur3-3* (9887405), and 35Spro:*XLT2:mur3-3* (11790956) were mapped to the *A. thaliana* genome with mapping ratios between 96.6% and 97.2% (Table 1). Similar numbers of genes were identified for WT (18123), *mur3-3* (18384), *xxt2mur3-3* (18242), *xxt5mur3-3* (18100), *xxt1xxt2mur3-3* (18101), and 35Spro:*XLT2:mur3-3* (18468). A total of 19,549 genes were expressed in all six plant lines of which 16,938 were overlapped (Supplementary file 2). Based on the RPKM data, only a small proportion of the genes were highly expressed. For example, only 61 of the 18123 WT genes had an expression value of more than 3 ($\log_{10}(\text{RPKM} + 1)$) (Fig. 2). All six libraries had similar RPKM distributions, which suggest that their transcript profiles are comparable (Fig. 2).

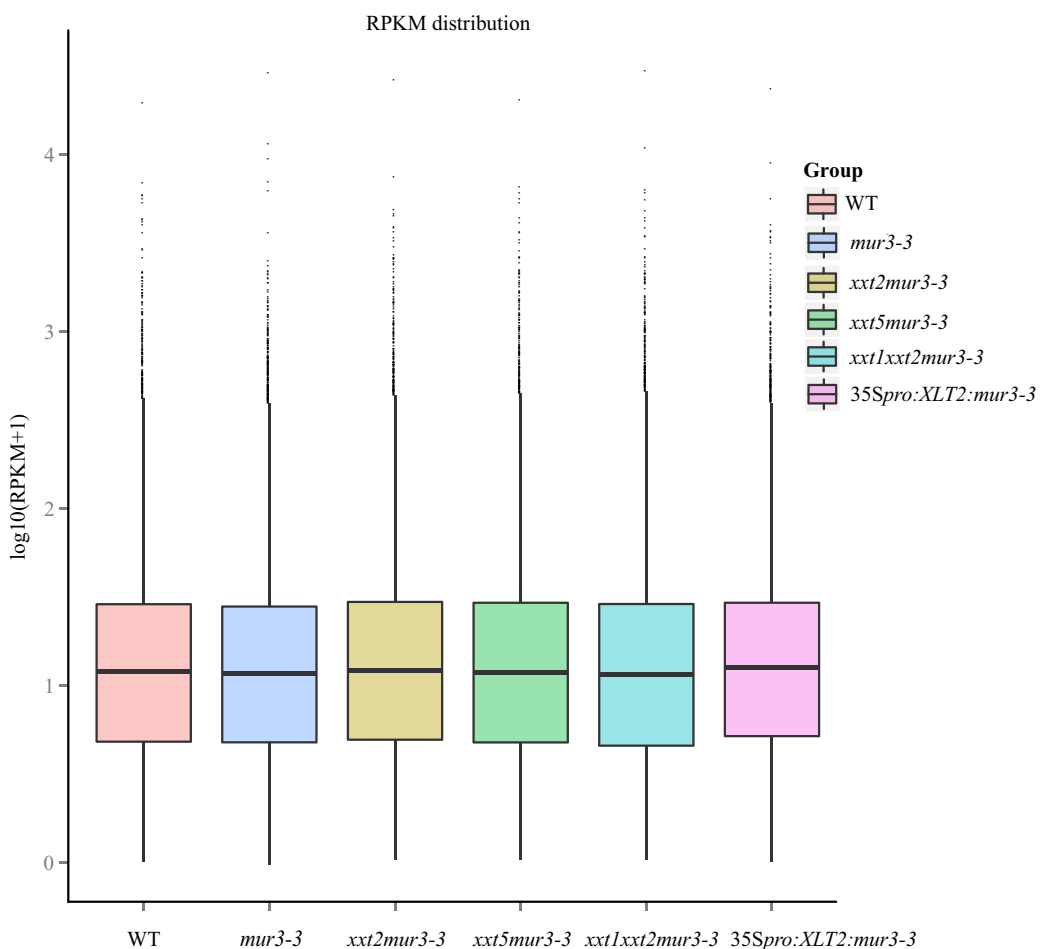


Fig. 2. The distribution of gene expression levels. The X axis represents the different plant lines and the Y axis is the \log_{10} (RPKM + 1) gene expression category (>0 and <5). Most of the genes are expressed at low levels. Only a small number of genes are highly expressed. All six libraries have similar expression patterns.

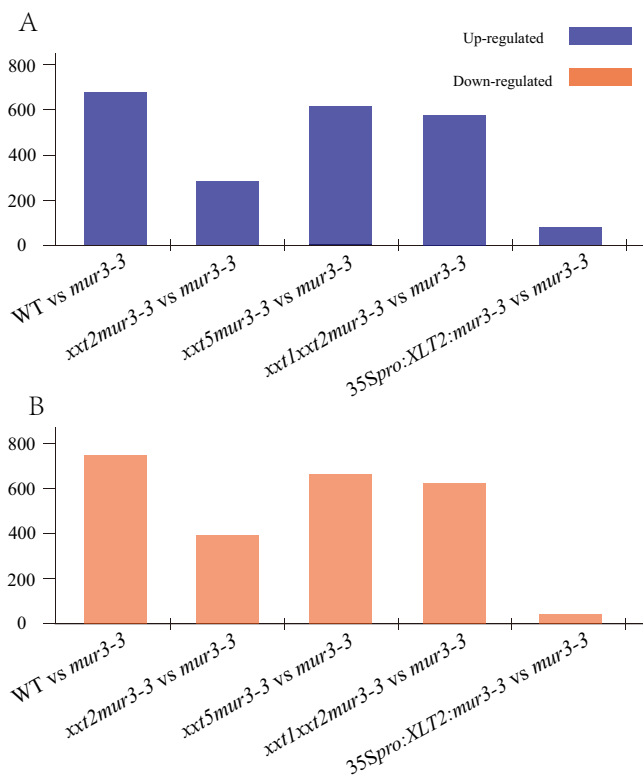


Fig. 3. The number of differently expressed genes in *mur3-3* compared with WT, *xxt2mur3-3*, *xxt5mur3-3*, *xxt1xxt2mur3-3* and *35Spro:XLT2:mur3-3*. A: Up-regulated DEGs in WT, *xxt2mur3-3*, *xxt5mur3-3*, *xxt1xxt2mur3-3* and *35Spro:XLT2:mur3-3* compared with *mur3-3*. B: Down-regulated DEGs in WT, *xxt2mur3-3*, *xxt5mur3-3*, *xxt1xxt2mur3-3* and *35Spro:XLT2:mur3-3* compared with *mur3-3*.

3.2. Overview of differentially expressed genes

To identify key genes involved in hypocotyl cell elongation in the xyloglucan-related mutants, we selected genes that are differentially expressed by using a corrected P-value <0.005 and an absolute value of \log_2 (fold change) ≥ 1 as the thresholds. Of the 1423 DEGs that differed between WT and *mur3-3*, 676 were up-regulated and 747 were down-regulated. 19 DEGs were uniquely expressed in WT and 50 in *mur3-3* (Fig. 3, Supplementary file 3). In the comparison between *xxt2mur3-3* and *mur3-3*, 283 DEGs were up-regulated and 392 were down-regulated. Only two genes were uniquely expressed in *mur3-3* (Fig. 3, Supplementary file 3). Similar numbers of DEGs were up- (613) or down-regulated (659) in *xxt5mur3-3* vs *mur3-3*, with 15 uniquely expressed in *xxt5mur3-3* and 17 in *mur3-3* (Fig. 3, Supplementary file 3). In the *xxt1xxt2mur3-3* vs *mur3-3* comparison 574 DEGs were up-regulated and 623 down-regulated, with 10 uniquely expressed in *xxt1xxt2mur3-3* and 38 in *mur3-3* (Fig. 3, Supplementary file 3). 79 DEGs were up-regulated and 42 down-regulated in the *35Spro:XLT2:mur3-3* vs *mur3-3* comparison, but no genes were uniquely expressed in either plant (Fig. 3, Supplementary file 3). Together the results of our analyses identified 887 up-regulated and 914 down-regulated genes whose expression was significantly different in the five comparisons. The up- and down-regulated genes can be clearly distinguished in the hierarchical clustering map which classified 1801 differential expression genes based on the RPKM value (Fig. 4). It is notable that *xxt1xxt2mur3-3* most closely resembles WT, as these two lines differed by only 99 DEGs (Supplementary file 3). Thus, the elimination of xyloglucan may have less effect on gene expression than the formation of a dysfunctional xyloglucan.

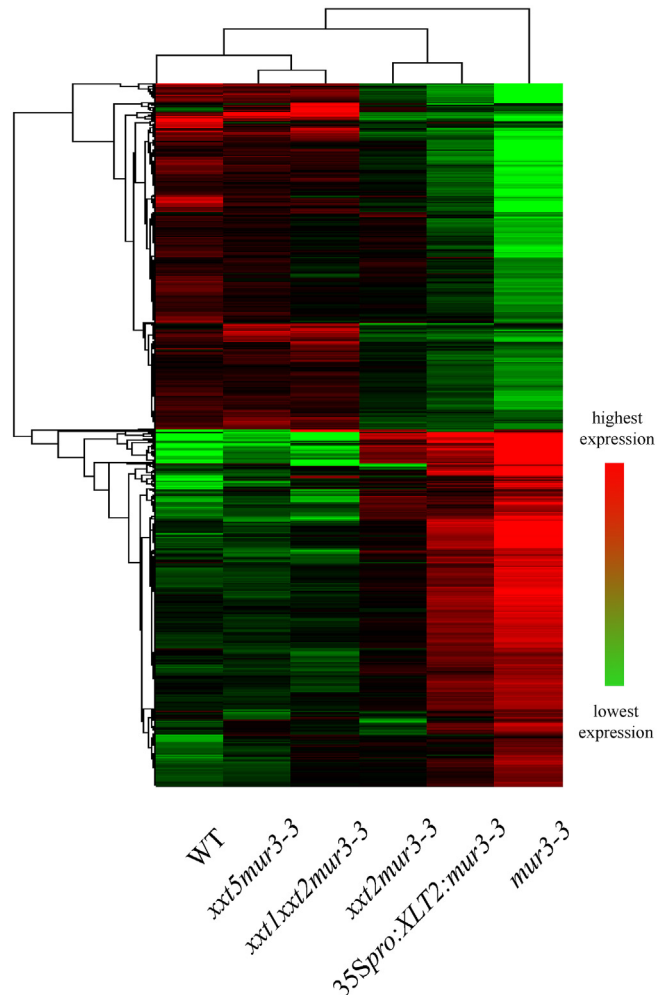


Fig. 4. Hierarchical cluster analysis of gene expression based on log ratio RPKM data ($\log_{10}(RPKM + 1)$). Green represents the lowest expression and red represents highest expression. Each column represents one of the six plant lines. Rows represent transcriptional units. (For interpretation of the references to color in this figure legend, the reader is referred to the web version of this article.)

3.3. GO and KEGG annotation of differentially expressed genes

We next used GO and KEGG assignments to annotate the differentially expressed genes to reveal their potential functions. Numerous significantly enriched GO terms of biological process, molecular function and cellular component were categorized in comparisons of *mur3-3* with WT (151), *xxt2mur3-3* (159), *xxt5mur3-3* (197), and with *xxt1xxt2mur3-3* (131) (Supplementary file 4, Fig. 5). No significantly enriched GO terms were categorized in the comparison of *mur3-3* with *35Spro:XLT2:mur3-3*. In the cellular component category, “plastid”, “plastid part”, “chloroplast”, and “organelle part” were significantly enriched ($p\text{-value} < 0.05$) in comparisons of *mur3-3* with WT, *xxt2mur3-3*, *xxt5mur3-3*, and with *xxt1xxt2mur3-3* (Supplementary file 4, Fig. 5). However, in the molecular function category, the top four enriched GO terms showed difference among these four comparisons. “Structural constituent of ribosome”, “structural molecule activity”, “oxygen binding”, and “transferase activity, transferring glycosyl groups” were dominantly enriched in WT vs *mur3-3*. However, the four most dominant enriched GO terms in *xxt1xxt2mur3-3* vs *mur3-3* were “hydrolase activity, acting on acid anhydrides, in phosphorus-containing anhydrides”, “hydrolase activity, acting on acid anhydrides”, “nucleoside-triphosphatase activity”, and “pyrophosphatase activity”. GO terms related to

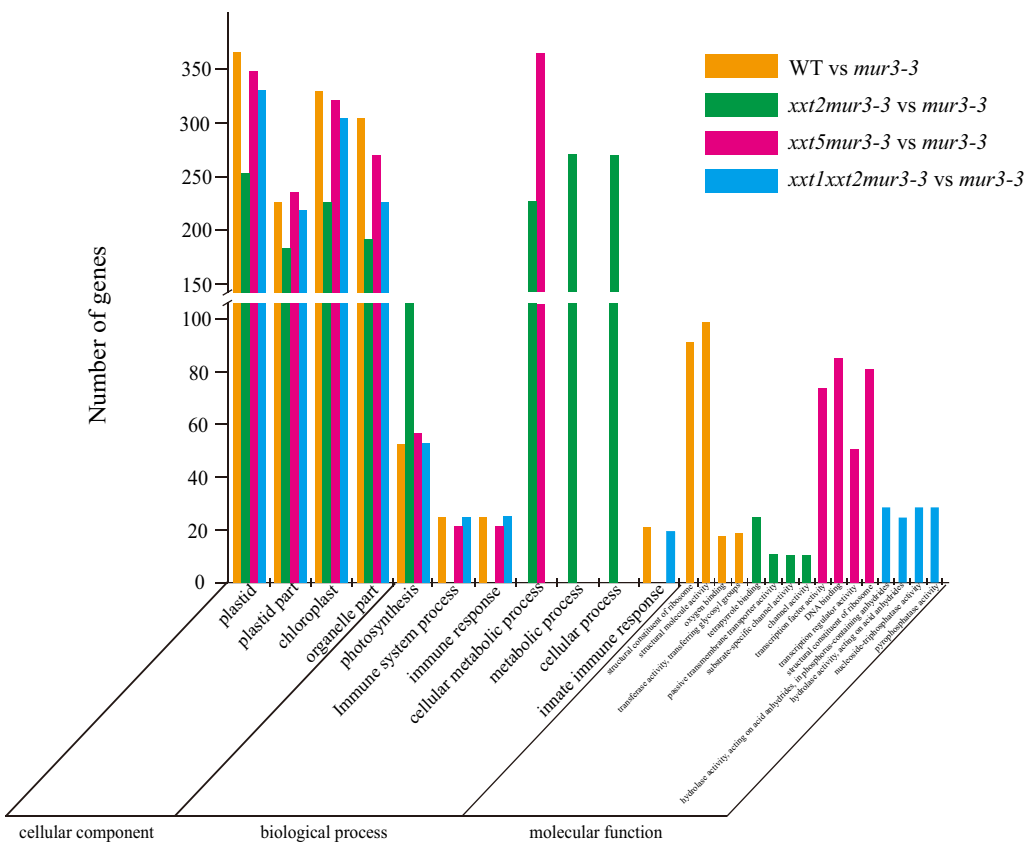


Fig. 5. Functional categories of DEGs in the Gene Ontology. The top four of the most significantly enriched (p -value <0.05) GO terms of biological process, molecular function and cellular component were analyzed in the comparisons of *mur3-3* with WT, *xxt2mur3-3*, *xxt5mur3-3* and *xxt1xxt2mur3-3*.

"tetrapyrrole binding", "passive transmembrane transporter activity", "substrate-specific channel activity" and "channel activity" were enriched in *xxt2mur3-3* vs *mur3-3*, which is a little difference with the most dominantly enriched four GO terms in *xxt5mur3-3* vs *mur3-3* "transcription factor activity", "DNA binding", "transcription regulator activity", and "structural constituent of ribosome" (Supplementary file 4, Fig. 5). In the biological process category, "immune system process", "immune response", "innate immune response", and "photosynthesis" were dominantly enriched both in WT vs *mur3-3* and *xxt1xxt2mur3-3* vs *mur3-3*. However, the top four enriched GO terms in *xxt5mur3-3* vs *mur3-3* were "photosynthesis", "immune system process", "immune response", and "cellular metabolic process". "Photosynthesis", "cellular metabolic process", and "cellular process" were dominantly enriched in *xxt2mur3-3* vs *mur3-3*, which showed a little difference with *xxt5mur3-3* vs *mur3-3* (Supplementary file 4, Fig. 5). In addition, we observed that the vast majority DEGs which enriched into immune response related GO terms were down-regulated in WT, *xxt1xxt2mur3-3* and *xxt5mur3-3* compared with *mur3-3* (Supplementary file 5).

DEGs from comparisons of *mur3-3* with WT (897), *xxt2mur3-3* (517), *xxt5mur3-3* (827), *xxt1xxt2mur3-3* (80) and 35Spro:XLT2:*mur3-3* (84) were mapped to 97, 79, 92, 87 and 31 KEGG pathways, respectively (Supplementary file 6). The top twenty significantly enriched KEGG pathways of each comparison are shown in Fig. S2. Metabolic pathways (average 22% of total mapped DEGs of every comparison) and the biosynthesis of secondary metabolites (average 12% of total mapped DEGs of every comparison) were most represented by the DEGs. Notably, we also observed that pathways related to "brassinosteroid biosynthesis" and "plant hormone signal transduction" were enriched in all five

comparisons. These annotations provide a valuable resource for investigating specific processes, functions and pathways related with cell elongation.

3.4. Differential expression genes involved in cell wall synthesis and modification

A total of 127 DEGs related to cell wall synthesis or modification showed different transcript levels in a comparison between *mur3-3*, WT and the four suppressor lines. This included genes encoding xyloglucan endotransglucosylase/hydrolases (XTHs), expansins, pectin methyl esterases (PMEs), arabinogalactan-proteins (AGPs), peroxidases, β -galactosidase, cellulose synthases and glucan endo-1,3-beta-glucosidase (Supplementary file 7). Comparisons of *mur3-3* with WT, *xxt2mur3-3*, *xxt5mur3-3*, *xxt1xxt2mur3-3* or 35Spro:XLT2:*mur3-3* identified 18 DEGs that included three XTHs (XTH4, XTH17 and XTH30), four AGPs (AGP5, AGP22, AGP24 and FLA13), three PMEs (PME3, PME16 and PME35) as well as EXPAs, PER53, BCB1 and COMT1. All of these genes were up-regulated in WT and the four suppressor lines compared with *mur3-3* except AGP5, PER53 and BCB1, which were down-regulated in WT and four suppressor lines compared with *mur3-3*. An additional 28 DEGs were detected in comparisons of *mur3-3* with WT, *xxt2mur3-3*, *xxt5mur3-3*, or *xxt1xxt2mur3-3* and included six AGPs (AGP1, AGP4, AGP7, AGP13, AGP14 and AGP21), two EXPAs (EXPAs6 and EXPAs11), two PMEs (PME34 and PME41), two PERs (PER64 and PER72), two BGALs (BGAL4 and BGAL8) as well as CESA2, CSLA9, XTH33, E13A, ENL2, GLPQ3, ATRABE1B. These DEGs were all up-regulated in WT and four suppressor lines compared with *mur3-3* except AGP1, ATRABE1B, EXPAs6, GLPQ3, PME41 and ENL2, which were down-regulated in WT and four suppressor lines compared with *mur3-3*. The remain-

Table 2Cell wall-related DEGs that differed significantly in comparisons of *mur3-3* with WT, *xxt2mur3-3*, *xxt5mur3-3*, *xxt1xxt2mur3-3* and *35Spro:XLT2:mur3-3*.

Type	Gene ID	log2.Fold_change.					Gene Name
		WT vs <i>mur3-3</i>	<i>xxt2mur3-3</i> vs <i>mur3-3</i>	<i>xxt5mur3-3</i> vs <i>mur3-3</i>	<i>xxt1xxt2mur3-3</i> vs <i>mur3-3</i>	<i>35Spro:XLT2:mur3-3</i> vs <i>mur3-3</i>	
Cell wall	AT5G53250	2.76	2.63	3.03	3.00	1.70	AGP22
	AT5G40730	2.43	1.96	2.33	2.36	1.20	AGP24
	AT1G35230	-5.29	-2.49	-4.48	-6.00	-1.69	AGP5
	AT5G20230	-6.93	-2.02	-4.82	-6.74	-1.73	SAG14
	AT5G63800	1.81	1.47	1.52	1.47	1.01	BGAL6
	AT1G76790	3.04	1.73	1.83	2.31	1.49	IGMT5
	AT1G08500	2.30	2.17	2.20	2.17	1.37	ENODL18
	AT2G40610	3.08	2.24	2.48	2.21	1.59	EXPA8
	AT5G44130	2.14	1.81	2.43	2.56	1.57	FLA13
	AT2G32990	2.03	1.65	1.81	1.99	1.65	GH9B8
	AT4G35160	2.84	2.28	2.75	3.21	1.65	ASMT
	AT5G06720	-2.92	-1.25	-2.68	-4.41	-1.23	PRX53
	AT2G43050	2.70	2.13	2.53	2.42	1.50	PMEPCRD
	AT3G14310	1.46	1.37	1.53	1.51	1.12	PME3
	AT3G59010	5.77	4.42	5.06	4.68	4.00	PME61
	AT1G65310	1.78	1.71	1.97	2.01	1.00	XTH17
	AT1G32170	2.68	2.36	2.36	2.16	1.45	XTH30
	AT2G06850	2.22	2.10	2.21	2.08	1.19	XTH4
TFs	AT1G04240	1.99	1.74	2.02	1.73	1.02	IAA3
	AT2G02820	2.72	2.19	2.48	2.22	2.11	MYB88
	AT2G29660	1.68	1.36	1.63	1.52	1.29	-
Chlorophyll <i>a-b</i> binding protein	AT1G29910	-3.77	-2.49	-3.54	-2.19	-1.42	LHCB1.2
	AT1G29920	-3.64	-3.96	-2.80	-2.07	-1.32	LHCB1.1
	AT1G29930	-2.99	-2.14	-2.87	-2.20	-1.11	LHCB1.3
	AT2G34430	-6.01	-4.30	-5.71	-4.13	-1.46	LHCB1.4
Hormone	AT5G35735	-1.72	-1.10	-1.88	-1.89	-1.03	-
	AT2G34500	2.63	2.07	2.09	2.10	1.32	CYP710A1
	AT2G34490	4.15	2.59	2.77	3.23	2.85	CYP710A1
	AT4G36380	2.07	1.73	1.82	1.95	1.28	ROT3
Protein kinase	AT5G37790	3.19	2.52	3.13	2.98	1.79	-
	AT3G15356	3.18	2.29	2.48	2.44	1.86	-
Aquaporin	AT4G23400	3.15	2.41	2.95	2.86	1.71	PIP1;5
	AT5G60660	4.62	4.15	4.59	4.77	3.19	PIP2;4
	AT4G17340	3.62	2.91	3.43	3.84	2.22	TIP2;2
	AT5G47450	2.64	2.55	2.91	3.14	1.43	TIP2;3

ing 81 cell wall-related DEGs were detected in other comparison pairs. 48 were up-regulated and 33 down-regulated in WT and four suppressor lines compared with *mur3-3*.

3.5. Differential expression genes involved in transcriptional factors

Transcription factors (TFs) have a key role in controlling gene expression in plants. We identified 130 differentially expressed TFs that belong to 24 different families including *AP2-EREBP*, *ARF/Aux-IAA*, *bZIP*, *MYB*, *WRKY*, *bHLH*, *C2H2*, *C2C2 (Zn)*, *NAC* and *Homeobox* (Supplementary file 8). Three TFs (*IAA3*, *MYB88* and a member of the *C2H2* gene family) were all up-regulated in WT and the four suppressor lines compared with *mur3-3*. 21 TFs were differentially expressed in comparisons between *mur3-3* and WT, *xxt2mur3-3*, *xxt5mur3-3* or *xxt1xxt2mur3-3*. Two *ARF/Aux-IAA* TFs (*IAA6* and *IAA17*), four *bHLH* TFs (*BH036*, *BH078*, *BH151* and *AT2G40820*), two *Homeobox* TFs (*HAT1* and *HAT2*), *MYB86* and *NAC100* were up-regulated in WT, *xxt2mur3-3*, *xxt5mur3-3* or *xxt1xxt2mur3-3* compared with *mur3-3*. By contrast, three *C2C2 (Zn)* TFs (*COL6*, *COL8* and *COL16*), two *C2H2* TFs (*ZAT8* and *ZAT12*) were down-regulated in WT, *xxt2mur3-3*, *xxt5mur3-3* or *xxt1xxt2mur3-3* compared with *mur3-3*. The remaining 106 TFs detected in comparisons between *mur3-3* and the other lines, included 83 that were up-regulated and 23 that were down-regulated in WT or some suppressor lines compared with *mur3-3*.

3.6. Detection of overlapped DEGs

The “cabbage-like” phenotype of *mur3-3* is suppressed by preventing xyloglucan synthesis (*xxt1xxt2mur3-3*) or by increasing the abundance of the XLXG subunit (*xxt2mur3-3*, *xxt5mur3-3* and *35Spro:XLT2:mur3-3*). To explore the underlying mechanism of suppression, we used Venn map statistical analysis to identify the overlapped DEGs (Fig. 6). A total of 102 overlapped DEGs were identified in comparisons of *mur3-3* with WT, *xxt2mur3-3*, *xxt5mur3-3*, *xxt1xxt2mur3-3* or *35Spro:XLT2:mur3-3*. 72 were up-regulated and 30 were down-regulated in WT and four suppressor lines compared with *mur3-3* (Supplementary file 9, Fig. 6A). 18 of these genes, including *XTH4*, *XTH17*, *XTH30*, *PME3*, *PME61*, *EXPA8*, *AGP5*, *AGP22* and *AGP24* are involved in cell wall biosynthesis or modification. Almost all of these cell wall-related DEGs were up-regulated (Table 2). 95% of the DEGs (115/121) detected in *35Spro:XLT2:mur3-3* vs *mur3-3* were also detected in WT vs *mur3-3* (Supplementary file 3).

A total of 550 overlapped DEGs were identified in comparisons of *mur3-3* with WT, *xxt2mur3-3*, *xxt5mur3-3* or *xxt1xxt2mur3-3*. 227 were up-regulated and 323 were down-regulated in comparisons with *mur3-3* (Supplementary file 9, Fig. 6B). 24 TFs and 46 cell wall-related DEGs, which include the 18 cell wall-related DEGs as described above, were identified. In addition, 6 auxin and brassinosteroids (BR) related genes, 9 protein kinase genes, 9 aquaporin genes and 18 chlorophyll *a-b* binding protein genes were identified. Notably, most of cell wall-related DEGs, TFs, hormone-related genes, protein kinase and aquaporin genes were up-regulated in

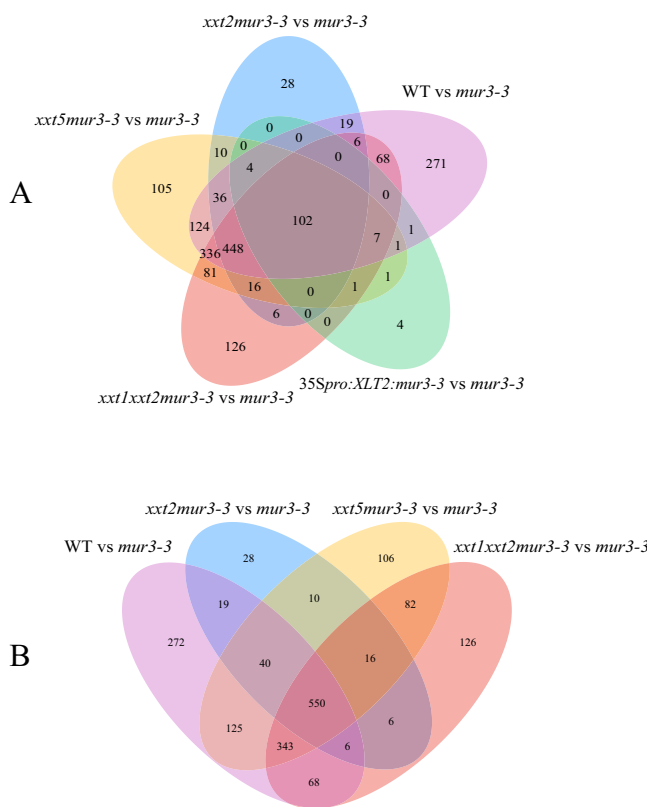


Fig. 6. DEGs showed in Venn diagram form. A: Venn diagram showing the numbers of overlapped DEGs detected in comparisons of *mur3-3* with WT, *xxt2mur3-3*, *xxt5mur3-3*, *xxt1xxt2mur3-3* and *35Spro:XLT2:mur3-3*. B: Venn diagram showing the numbers of overlapped DEGs detected in comparisons of *mur3-3* with WT, *xxt2mur3-3*, *xxt5mur3-3* and *xxt1xxt2mur3-3*. The Venn diagrams include both up- and down-regulated genes.

WT and suppressor lines compared with *mur3-3*, whereas all of the chlorophyll a-b binding protein genes were down-regulated in WT and suppressor lines compared with *mur3-3*. Visualization of the 550 DEGs using MapMan revealed a clustering of these genes into metabolic pathways (Fig. 7A), regulatory processes (Fig. 7B), and biotic stress processes (Fig. 7C). Most cell wall-related genes, protein modification genes, hormone-related genes and PR-protein genes were up-regulated relative to *mur3-3*, while all the light reaction related genes were down-regulated relative to *mur3-3*.

3.7. Conserved promoter motifs analysis

Conserved motifs in gene promoters typically indicate related functions of a cluster of genes. To explore the potential variance of gene function between the up- and down-regulated DEGs, we analyzed the conserved promoter motifs of the 102 overlapped DEGs detected in the comparison pairs of WT, *xxt2mur3-3*, *xxt5mur3-3*, *xxt1xxt2mur3-3* and *35Spro:XLT2:mur3-3* vs *mur3-3*. A total of 27 and 12 conserved promoter motifs were significantly enriched in up- and down-regulated DEGs (P -value < 0.05), respectively (Supplementary file 10). A TATA-box, CARGC8GAT, T-box promoter, Ibox promoter, ABRE-like binding site and Z-box promoter motifs were detected in most of the up- and down-regulated DEGs. 21 and 6 conserved promoter motifs were specifically detected in up- and down-regulated DEGs, respectively. For example, MYB1AT, the MYB4 binding site and W-box promoter motifs, GAREAT, MYCATERD1 and AtMYC2 BS in RD22 conserved promoter motifs were specifically enriched in up-regulated DEGs. SV40 core promoter motif, ACCTABREMOTIFA2OSEM and GADOWNAT were enriched in down-regulated DEGs.

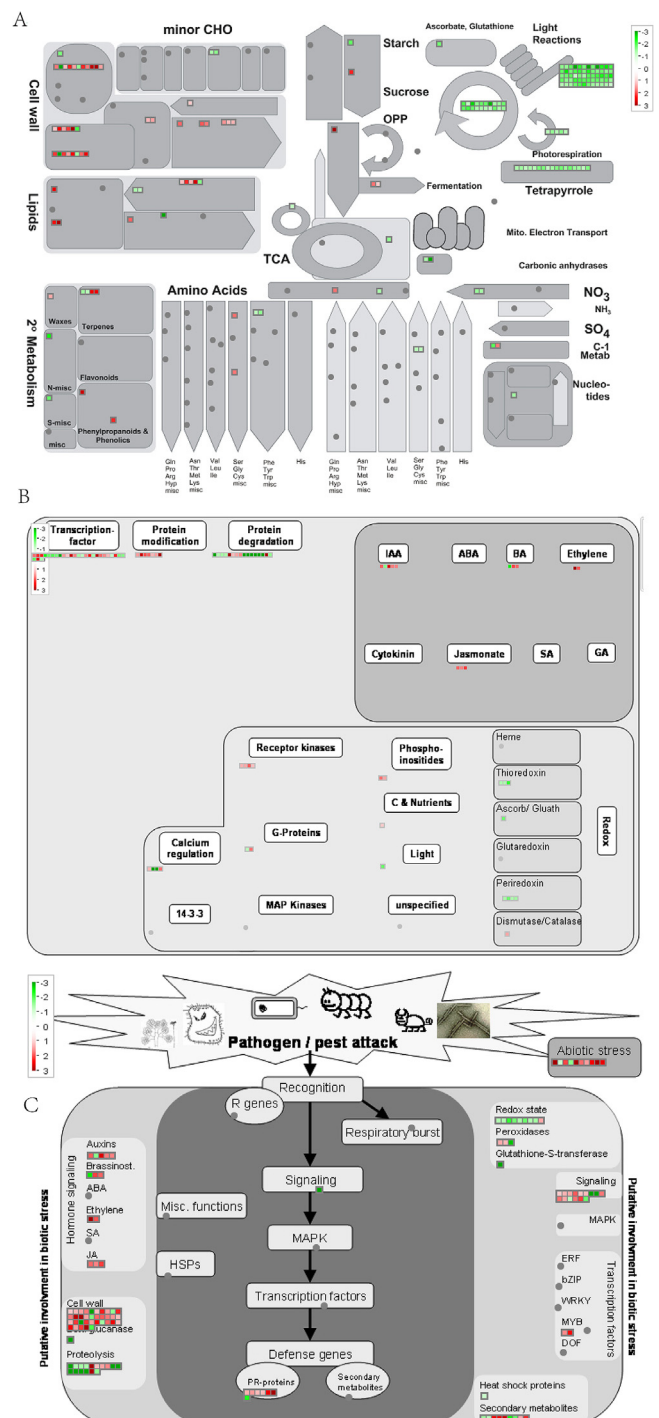
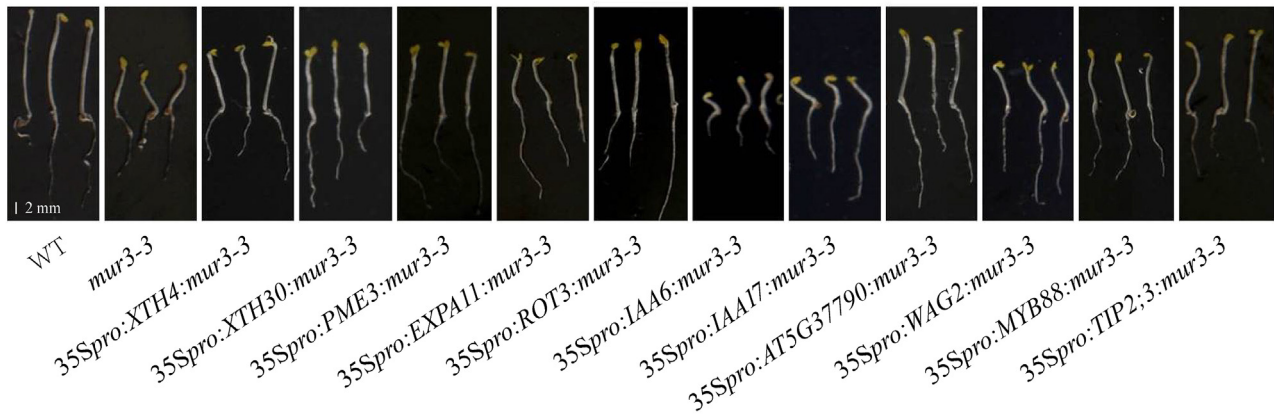


Fig. 7. Overview of 550 overlapped DEGs involved in different metabolic and regulatory processes visualized by MapMan. A: Overview display of DEGs assigned to metabolism. CHO, carbohydrates; OPP, oxidative pentose phosphate pathway; TCA, tricarboxylic acid cycle. B: Overview display of DEGs assigned to regulatory processes. C: Overview display of DEGs assigned to biotic stress processes. Genes significantly up- and down-regulated in WT and suppressor lines compared with *mur3-3* are indicated in red and green, respectively. Scale bars display log₂-fold changes. (For interpretation of the references to colour in this figure legend, the reader is referred to the web version of this article.)

3.8. Complementation test

We selected 11 DEGs down-regulated in *mur3-3* relative to WT and the four suppressor lines to investigate their role in cell elongation. The DEGs encode cell wall-related proteins, TFs,

A



B

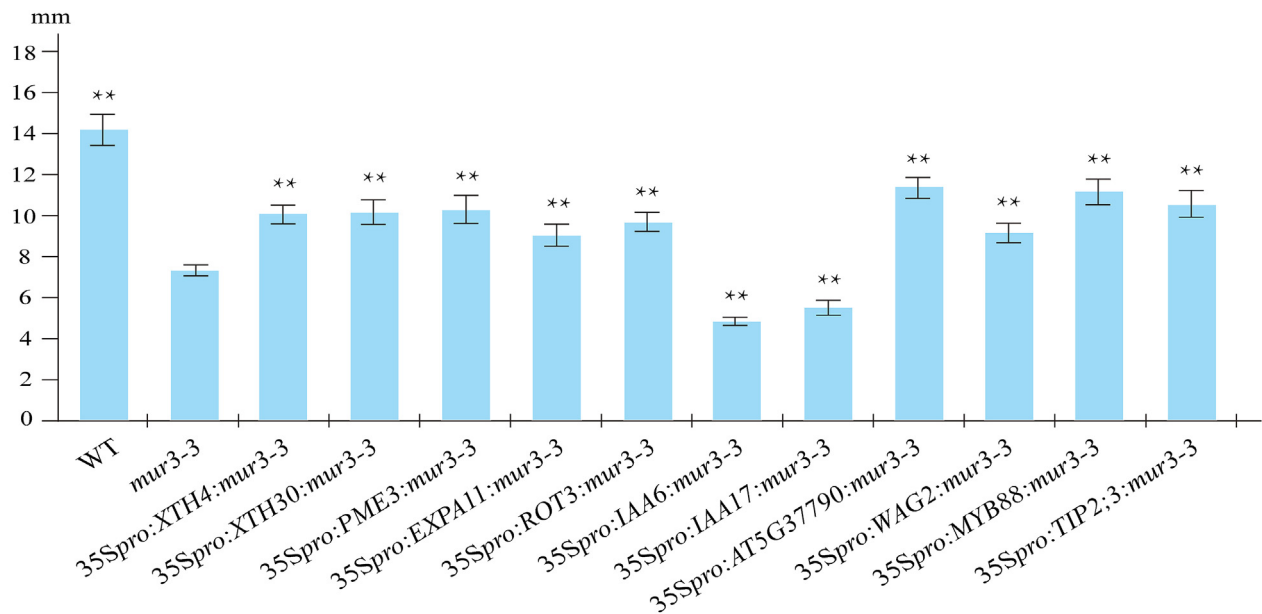


Fig. 8. Overexpression of selected genes rescues the short hypocotyl phenotype of the *mur3-3* mutant. A: The hypocotyl phenotypes of *mur3-3* lines over expressing *XTH4*, *XTH30*, *PME3*, *EXPA11*, *ROT3*, *IAA6*, *IAA17*, *WAG2*, *AT5G37790*, *MYB88* or *TIP2;3*. B: Hypocotyl length of WT, *mur3-3* and transgenic lines. Between 10 and 15 hypocotyls were measured for each transgenic line. Data shown are average +/− SD. (Student's two-tailed *t*-test with *mur3-3*; ** *P* < 0.01).

hormone-related proteins, protein kinases and aquaporins (Supplementary file 11). Each DEG was overexpressed in *mur3-3* to determine if they rescued the *mur3-3* phenotype. At least 20 transgenic lines were generated for each gene. The aerial portions of the transgenic lines and *mur3-3* were indistinguishable (data not shown) suggesting that the leaf growth phenotype cannot be rescued by expressing any of these genes individually. Two transgenic lines (*35Spro:IAA6:mur3-3* and *35Spro:IAA17:mur3-3*) had shorter hypocotyls than *mur3-3* (Fig. 8). By contrast, the *mur3-3* short hypocotyl phenotype was partially rescued by overexpressing four cell wall-related genes (*XTH4*, *XTH30*, *PME3* and *EXPA11*), a TF (*MYB88*), a hormone-related gene (*ROT3*), two protein kinase genes (*AT5G37790* and *WAG2*) and a aquaporin gene (*TIP2;3*) (Fig. 8). Thus, differences may exist in cell elongation mechanism in adult plants and in hypocotyls.

3.9. Co-expression networks underlying the hypocotyl elongation

The 46 cell wall-related genes, 24 TFs, 6 hormone-related genes, 9 kinase genes, 9 aquaporin genes and 18 chlorophyll a-b binding protein genes showed different expression levels in *mur3-3* compared with WT, *xxt2mur3-3*, *xxt5mur3-3* or *xxt1xxt2mur3-3* (Supplementary file 9). Complementation test showed that elevating some of these genes that were down-regulated in *mur3-3* partially rescued the hypocotyl phenotype (Fig. 8). We constructed a global co-expression network of these genes by using WGCNA to explore the potential correlations of these DEGs with the regulation of cell elongation. These results showed that most of the cell wall-related genes including *XTH33*, *EXPA6*, *PRX53*, *BGL2* and *ENODL2* co-expressed with TFs, hormone-related genes and genes encoding protein kinases, aquaporins, and chlorophyll a-b binding proteins (Supplementary file 12, Fig. 9).

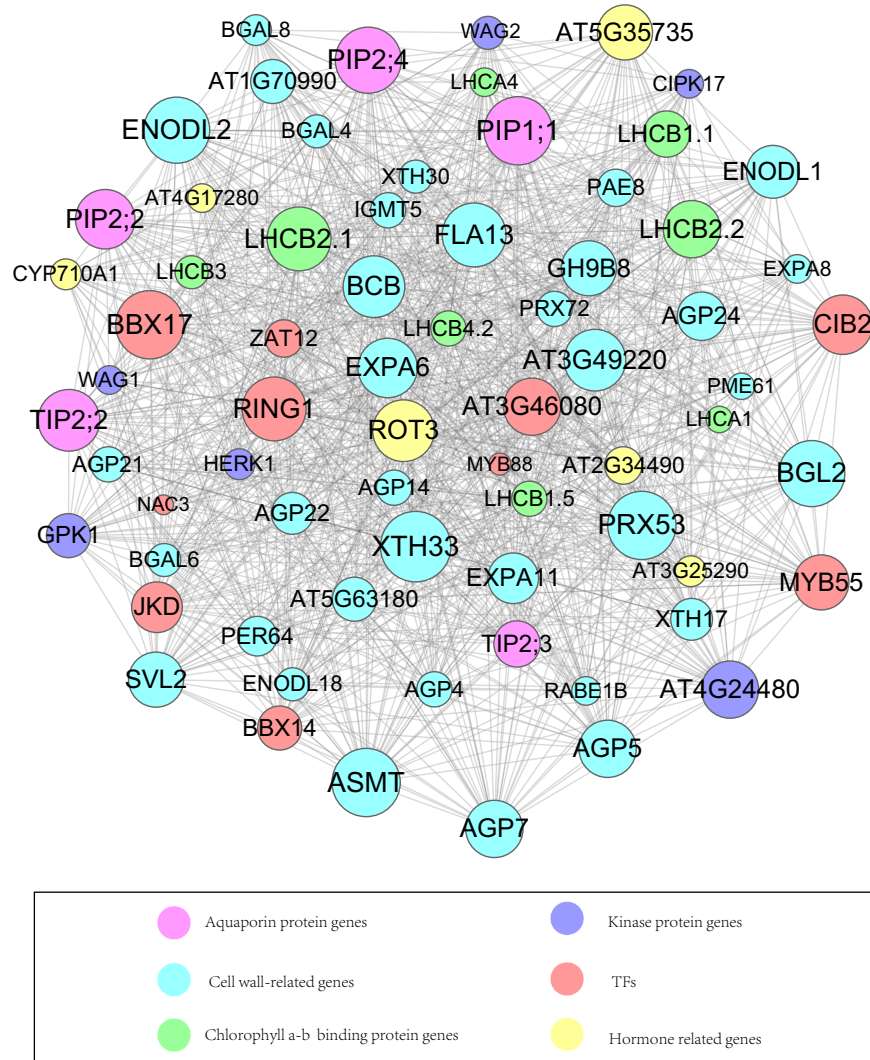


Fig. 9. The weighted co-expression network of differentially expressed genes including cell wall-related genes, TFs, hormone genes, protein kinase genes, aquaporins and chlorophyll a-b binding protein genes. The different color represents different types of genes and the size of the circle represents the quantity of connection joints with other genes.

In addition, among these co-expression DEGs, the TFs *MYB55* (*AT4G01680*), *BBX17* (*AT1G49130*), *RING1* (*AT5G10380*) and *AT3G46080*, hormone-related genes *CYP710A2* (*AT2G34490*) and *ROT3* (*AT4G36380*) had expression patterns (WT > *xxt5mur3-3>xxt2mur3-3>mur3-3*) similar to genes encoding aquaporin proteins *PIP1;1* (*AT3G61430*), *PIP2;2* (*AT2G37170*), *PIP2;4* (*AT5G60660*) and *TIP2;2* (*AT4G17340*) and kinase proteins *AT3G15356* and *GPK1* (*AT3G17420*) (Supplementary file 9, Supplementary file 12). The expression level trend of these DEGs is correlated with the abundance of the XLXG subunit in the plants, indicating that expressions of the DEGs are correlated with the presence of the dysfunctional xyloglucan. This result further supports our previous conclusion that the *mur3-3* phenotype results from the reduced amounts of the XLXG subunit.

3.10. Quantitative real-time PCR analysis

To validate the differential DEG data obtained by Illumina Hiseq 2000/2500 platform sequencing we used qRT-PCR analyses of eleven cell-wall related DEGs, one TF and three protein kinase DEGs selected randomly from the 550 overlapped DEGs detected from comparisons of *mur3-3* with the other plants (Fig. 6B). The qRT-PCR expression patterns of these fifteen DEGs exhibited similar expres-

sion patterns with DGE-seq (Fig. 10A). Linear regression analysis showed a significant correlation ($R^2 = 0.9323$), which indicates good reproducibility between transcript abundance generated by DGE-seq and the expression profiles obtained from the qRT-PCR data (Fig. 10B).

4. Discussion

To our knowledge, our study is the first to provide a large-scale assessment of the transcriptomes of plants carrying mutations in GTs known to be involved in the synthesis of xyloglucan. This study provides a foundation for understanding the underlying mechanism of how changes in xyloglucan structure affect cell elongation.

Cell wall synthesis and remodeling are key steps in the assembly of a functional cell wall and thus have important roles in regulating cell elongation and division. Several genes involved in these two processes including those encoding glycoside hydrolases, expansins, carbohydrate lyases, peroxidases, laccases, AGPs, fasiclin AGPs (FLAs), PMEs, PMEIs, GHs, XTHs, beta-galactosidases, cellulose and callose synthase genes (Supplementary File 7) were identified in our study and found to be differentially expressed.

Xyloglucan and pectin have been proposed to have key roles in determining the mechanical properties of the primary cell walls

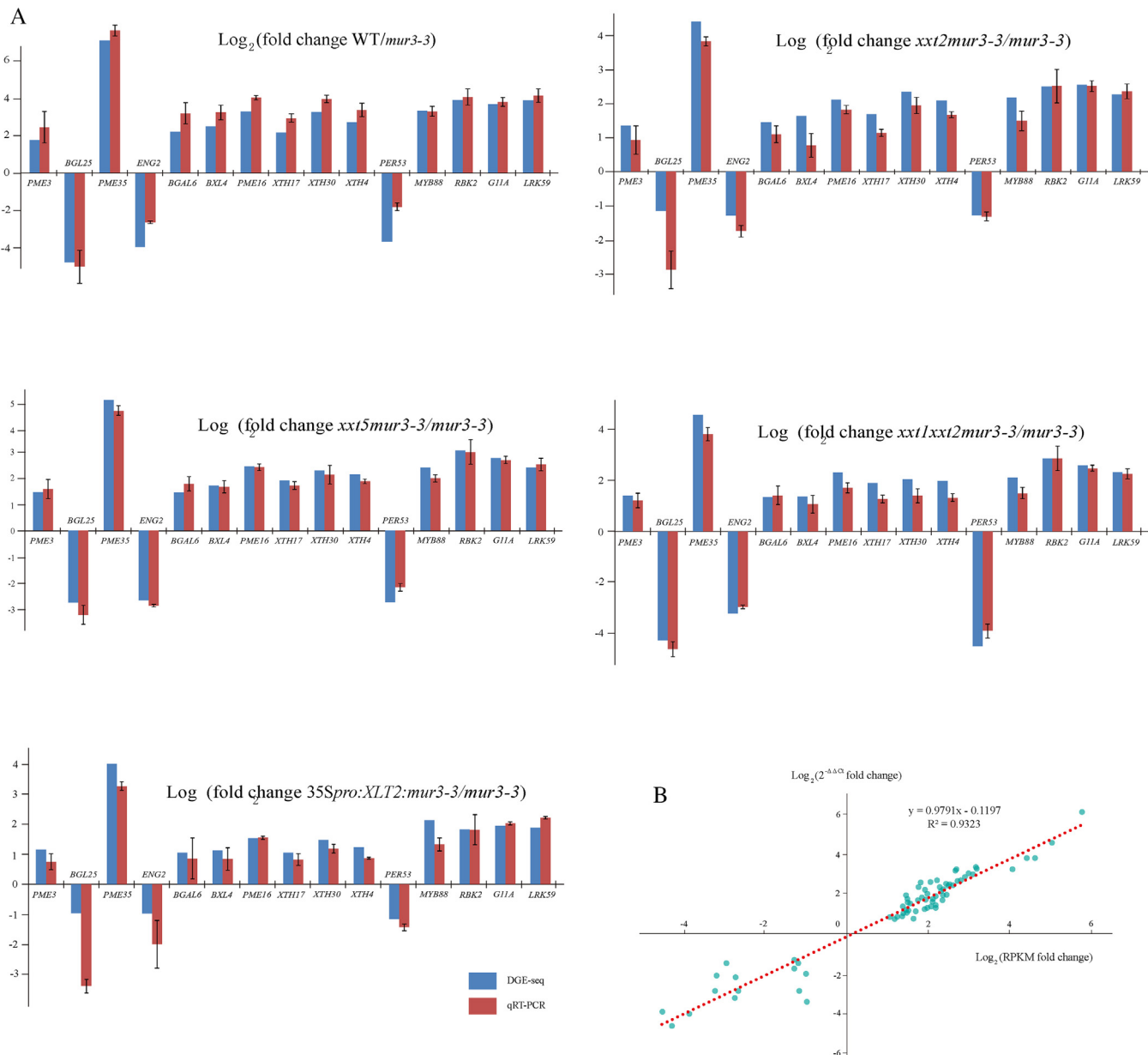


Fig. 10. Comparison of the changes in the abundance and expression levels of selected genes. A: The relative expression values representing \log_2 (fold change) among comparisons of *mur3-3* with WT and four suppressor lines. RPKM values were used in DGE-seq and $2^{-\Delta\Delta CT}$ values were used in qRT-PCR for fold-change calculation. B: Coefficient analysis between gene expression ratios obtained from DGE-seq and qRT-PCR data.

[42] and thus are important for normal cell elongation. Thus, it is not unexpected that genes encoding PMEs (5) and XTHs (3) were present as overlapped DEGs in pairwise comparisons of WT vs *mur3-3*, *xxt2mur3-3* vs *mur3-3*, *xxt5mur3-3* vs *mur3-3* and *xxt1xxt2mur3-3* vs *mur3-3*. Many of these genes were also identified to have important roles during cell elongation and hypocotyl growth in transcriptomics or proteomics studies of elongating *Arabidopsis* hypocotyls [43–45]. Our complementation test supports this notion since overexpression of *XTH4*, *XTH30*, *PME3* and *EXPA11* partially rescued the length of *mur3-3* hypocotyls (Fig. 8).

It is intriguing that the *xxt1xxt2mur3-3* mutant, which lacks xyloglucan in its cell walls has gene expression profiles that most closely resemble WT (Supplementary file 2). This adds support to our previous proposal that the absence of xyloglucan has a less deleterious effect on plant growth than the presence of xyloglucan with a dysfunctional structure [19]. In comparison to *mur3-3*, the expression level of more than 80% of DEGs in WT vs *mur3-3* reverted

to WT levels in *xxt2mur3-3*, *xxt5mur3-3*, *xxt1xxt2mur3-3* and even *35Spro:XLT2:mur3-3* (Supplementary file 13), which suggests that in these suppressor lines the *mur3-3* phenotypes are suppressed through similar pathways and that the galactose-deficient xyloglucan or galactose-deficient xyloglucan oligosaccharides signal the cellular changes and thus affect cell elongation.

4.1. Auxin and BR may contribute to *mur3-3* hypocotyl elongation defect

Auxin regulates many aspects of plant growth and development [46]. This hormone controls transcription by rapidly modulating the levels of short-lived Aux/IAA proteins [47]. In the SCFTIR1/AFB-auxin-Aux/IAA auxin signaling transduction model, auxin triggers Aux/IAA degradation and de-repression of ARF activity, enabling promoter activation for gene expression [47]. In our study, we found that *IAA3*, *IAA6* and *IAA17* were significantly down-regulated

in *mur3-3* compared with WT (Supplementary file 8) together with the down-regulation of *XTHs*, *PMEs* and *AGPs* (Table 2, Supplementary file 7). It is notable that the expression levels of the three *Aux/IAAs* genes in the *mur3-3* suppressor lines revert to WT levels (Supplementary file 2). Several hormones, including auxin and BR, have been proposed to mediate their effects on cell elongation via alteration of wall architecture [48]. Thus, it is possible that the changes in cell wall-related DEGs are regulated by changes in IAA.

Several studies have reported that seedlings of the gain-of-function mutants *shy2-2/iaa3*, *shy1/iaa6* and *axr3/iaa17* have short hypocotyls and curled leaves and that genes encoding *XTHs*, *PMEs*, and *AGPs* are repressed [49–52]. The *XTH17*, *AGP22*, and *AGP4* genes that are repressed in *axr3/iaa17* were also repressed in *mur3-3* compared with WT. Additional experiments are required to verify if gain-of-function of *IAAs* and knock down of *IAAs* inhibit plant growth through similar pathways. Notably, our overexpression experiments showed that *IAA6* and *IAA17* do not rescue, but enhance the *mur3-3* short hypocotyl phenotype further implicating the complex regulatory mechanism of auxin during hypocotyl elongation.

Brassinosteroids are a class of hormones that regulate numerous aspects of plant growth and development [53]. These hormones are perceived by *BRI1*, which then activates the TFs *BZR1/2* through inhibition of *BIN2*, a GSK3-like kinase. *BZR1/2*, also regulates numerous other genes including many involved in cell wall-biosynthesis and remodeling [54,55]. Previous studies reported that many BR biosynthetic mutants including *det2*, *dim*, *dwarf1*, *cbb1*, *brd1*, *lka* and *lkb* have short hypocotyls, petioles, and stems, and small leaves [56–59] suggesting that the dwarfism in BR biosynthetic and BR-insensitive mutants results from reduced cell elongation. Consistent with previous studies, we found that three genes involved in sterol biosynthetic (*ROT3*, *CYP710A2* and *CYP710A1*) were down-regulated in *mur3-3* compared with WT, *xxt2mur3-3*, *xxt5mur3-3*, *xxt1xxt2mur3-3* and *35Spro:XLT2:mur3-3*. Since most BR biosynthetic genes are believed to be under negative feedback control by BR signaling [48], it is possible that the elongation defects in *mur3-3* result in part from elevated BR signaling. A previous study has reported that inhibition of PME activity leads to a reduction of pectate in the cell wall, which may trigger BR signaling. Elevated BR signaling is the main cause of the abnormal phenotype when PME activity is disturbed [48]. Consistent with such studies, we found that *PME3*, *PME16*, *PME34* and *PME35* were all down-regulated in *mur3-3* relative to WT (Table 2). Thus, in *mur3-3*, the reduced expression of *PMEs* may result in elevated BR signaling which then leads to the “cabbage-like” phenotype. Evidence to support this notion was obtained by complementation tests, which showed that the short hypocotyl phenotype of *mur3-3* is partially rescued in the *35Spro:PME3:mur3-3* and *35Spro:ROT3:mur3-3* transgenic lines (Fig. 8).

4.2. TFs and receptor kinase proteins that possibly responsible for hypocotyl elongation defect in *mur3-3*

Plasma membrane-localized receptor-like kinases (RLKs) have been suggested to be the primary candidates for sensing changes in cell wall integrity [23]. Wall associated kinases (WAKs) that have a highly conserved serine/threonine protein kinase domain on their cytoplasmic domain and the *Catharanthus roseus* RLK1 (CrRLK1) like protein family are two of the best-studied potential cell wall integrity receptors [60,61]. In our study, we identified 9 kinases in the 550 overlapped genes, including the *CrRLK1-like* family member *HERCULES1* (*HER1*) and 8 serine/threonine protein kinases. Further experiments are required to verify whether these two RLKs are involved in sensing changes in cell wall mechanics that result from altered xyloglucan structure. Indeed, our data showing that overexpression *WAG2* or *At5g37790* partially rescued the *mur3-3*

short hypocotyl phenotype suggests that kinases do have a role in xyloglucan signal sensing and transduction.

Identifying TFs responsible for the *mur3-3* short hypocotyl phenotype is required to elucidate the underlying mechanism that control cell elongation. In our study, several TFs gene families including *bHLH*, *MYB*, *homeobox*, *BZR*, *NAC*, *Sigma70-like* and the *tri-helix* family were identified (Supplementary file 8). Overexpression of *MYB88* partially rescued the *mur3-3* hypocotyl phenotype, suggesting that one or more of these TFs are potential candidates for the cell elongation defect observed in *mur3-3* hypocotyls.

4.3. Aquaporins may facilitate cell elongation

Plant cell growth requires the irreversible increase in the surface area of the cell wall. This process requires an internal turgor pressure, which is generated by water uptake into the cell [62–64]. To maintain turgor during cell wall expansion, water movement through cell membranes is enabled by water channels referred to as aquaporins [65]. Aquaporins are integral membrane proteins that form pores which facilitate water transport at a rate higher than diffusion. The increased accumulation of aquaporins likely allows water to enter a cell at an accelerated rate, leading to a higher turgor pressure that drives cell elongation. Consistent with this hypothesis, a previous report showing that transgenic tobacco overexpressing an *Arabidopsis* plasma membrane aquaporin gene (*PIP1b*), are taller than WT as a consequence of the increased length and number of internodes [66]. We found that seven *PIPs* and two *TIPs* aquaporin genes were up-regulated in WT and the four suppressor lines compared with *mur3-3* (Supplementary file 9), suggesting that these proteins may help maintain a higher turgor pressure to facilitate the normal cell elongation. This notion was supported by complementation tests showing that overexpressing *TIP2;3* in *mur3-3* promoted cell elongation. On the other hand, it has been reported that in *Arabidopsis* roots auxin suppresses the transcription of several *PIP* and *TIP* genes including *PIP1;1*, *PIP1;5*, *PIP2;1*, *PIP2;2*, *PIP2;4*, *PIP2;7*, *TIP2;2* and *TIP2;3* [67]. These 8 genes also appeared in the 550 overlapped DEGs and were down-regulated in *mur3-3* compared with WT and the suppressor lines (Supplementary file 9). Thus we suggest that the lower expression of these aquaporin genes in *mur3-3* is due to an elevated auxin signal since *IAA3*, *IAA6*, *IAA17* were significantly down-regulated in *mur3-3*.

4.4. The elevated immune response in *mur3-3*

Plant cell walls serve as physical barriers against pathogen entry, however, phytopathogenic fungi, bacteria, and nematodes secrete enzymes that can break the integrity of the plant cell wall [68]. Pectic enzymes, including polygalacturonases (PGs), pectate lyases (PELs) and PMEs are typically the first cell wall degrading enzymes secreted by fungal and bacterial pathogens during the initial stages of infection [69]. Xyloglucan, the predominant hemicellulosic polysaccharide in the primary walls of dicots and non-graminaceous monocots, is fragmented by microbial xyloglucan-specific endoglucanases (XEGs) [68]. Plant cells have membrane-localized receptors that perceive the molecules generated by the cell wall-degrading enzymes in damaged tissues [70] and activate plant immune responses [71,72]. In our study, we found that several GO terms, including “immune system process”, “immune response” and “innate immune response” were enriched in *mur3-3* compared with WT or *xxt1xxt2mur3-3*. The latter two terms were also enriched in *mur3-3* compared with *xxt5mur3-3* (Supplementary file 4, Fig. 5). Most of the DEGs enriched in these GO terms were up-regulated in *mur3-3* compared with WT or suppressor lines (Supplementary file 5) indicating that the dysfunctional xyloglucan in *mur3-3* activates severe immune response, although further studies are needed to clarify the underlying mechanism.

The esterification status of pectin can affect cell wall degradability by microbial enzymes. Genetic and molecular evidence has indicated that pectin methyl-esterification has a critical role in a plant's defence against pathogens [73]. Studies in *Arabidopsis* and wheat have shown that lower levels of PME activity is correlated with an increase of pectin esterification and a concomitant decrease in susceptibility to the pathogen [74,75]. In our data, several genes encoding PMEs were down-regulated in *mur3-3* compared with WT and the suppressor lines (Supplementary file 7). The constitutive resistance of *mur3-3* petioles to infection by *H. parasitica* [21] may result from elevated expression of these immune response genes and the decreased expression of PME genes.

5. Conclusions

Our DGE-seq data provides insights into the molecular basis of how modifying a cell wall polysaccharide may lead to reduced cell elongation. Structural changes to cell wall xyloglucan must be perceived and then relayed to the cytosol where they cause changes in the expression of numerous genes related to cell wall metabolism, TFs, hormones, receptor kinases and aquaporins. Our study illustrates how combining knowledge of mutant cell wall structure with gene expression data and bioinformatics provides new insight into the molecular mechanism underlying plant cell elongation.

Competing interests

The authors declare that they have no competing interests.

Authors' contributions

This study was conceived by ZX, DS, TN and YK. The preparation of plant material was conducted by DS, TN and MW. Complementation test were finished by MW. ZX, MW, GZ and YK contributed to the data analysis, the bioinformatics analysis and manuscript preparation. MAO and MGH revised the manuscript. All authors have read and approved the final manuscript.

Acknowledgements

This work was supported by the National Natural Science Foundation of China (31470291, 31670302), the National Key Technology R&D Program (2015BAD15B03-05), the Elite Youth Program of CAAS (to YK), the Taishan Scholar Program of Shandong (to GZ) and The Division of Chemical Sciences, Geosciences, and Biosciences, Office of Basic Energy Sciences of the U.S. Department of Energy through grant DE-FG02-12ER16324 (to MAO).

Appendix A. Supplementary data

Supplementary data associated with this article can be found, in the online version, at <http://dx.doi.org/10.1016/j.plantsci.2017.01.005>.

References

- [1] M.A. O'Neill, W.S. York, *The Composition and Structure of Plant Primary Cell Walls*, The Plant Cell Wall, Blackwell Publishing/CRC Press, Ithaca, New York, 2003, pp. 1–54.
- [2] M.J. Pena, A.G. Darvill, S. Eberhard, W.S. York, M.A. O'Neill, Moss and liverwort xyloglucans contain galacturonic acid and are structurally distinct from the xyloglucans synthesized by hornworts and vascular plants, *Glycobiology* 18 (2008) 891–904.
- [3] R.M. Perrin, Z. Jia, T.A. Wagner, M.A. O'Neill, R. Sarria, W.S. York, N.V. Raikhel, K. Keegstra, Analysis of xyloglucan fucosylation in *Arabidopsis*, *Plant Physiol.* 132 (2003) 768–778.
- [4] M. Hoffman, Z. Jia, M.J. Peña, M. Cash, A. Harper, A.R. Blackburn II, A. Darvill, W.S. York, Structural analysis of xyloglucans in the primary cell walls of plants in the subclass Asteridae, *Carbohydr. Res.* 340 (2005) 1826–1840.
- [5] J.K. Jensen, A. Schultink, K. Keegstra, C.G. Wilkerson, M. Pauly, RNA-Seq analysis of developing nasturtium seeds (*Tropaeolum majus*): identification and characterization of an additional galactosyltransferase involved in xyloglucan biosynthesis, *Mol. Plant* 5 (2012) 984–992.
- [6] M. Madson, C. Dunand, X. Li, R. Verma, G.F. Vanzin, J. Caplan, D.A. Shoue, N.C. Carpita, W.-D. Reiter, The *MUR3* gene of *Arabidopsis* encodes a xyloglucan galactosyltransferase that is evolutionarily related to animal exostosins, *Plant Cell* 15 (2003) 1662–1670.
- [7] R.M. Perrin, A.E. DeRocher, M. Bar-Peled, W. Zeng, L. Norambuena, A. Orellana, N.V. Raikhel, K. Keegstra, Xyloglucan fucosyltransferase, an enzyme involved in plant cell wall biosynthesis, *Science* 284 (1999) 1976–1979.
- [8] S. Vuttipongchaikij, D. Brocklehurst, C. Steele-King, D.A. Ashford, L.D. Gomez, S.J. McQueen-Mason, *Arabidopsis* GT34 family contains five xyloglucan alpha-1, 6-xylosyltransferases, *New Phytol.* 195 (2012) 585–595.
- [9] D.M. Cavalier, K. Keegstra, Two xyloglucan xylosyltransferases catalyze the addition of multiple xylosyl residues to cellobhexaose, *J. Biol. Chem.* 281 (2006) 34197–34207.
- [10] A.T. Culbertson, Y.H. Chou, A.L. Smith, Z.T. Young, A.A. Tietze, S. Cottaz, R. Faure, O.A. Zabotina, Enzymatic activity of xyloglucan xylosyltransferase 5, *Plant Physiol.* 171 (2016) 1893–1904.
- [11] L. von Schantz, F. Gullfot, S. Scheer, L. Filonova, L. Cicortas Gunnarsson, J.E. Flint, G. Daniel, E. Nordberg-Karlsson, H. Brumer, M. Ohlin, Affinity maturation generates greatly improved xyloglucan-specific carbohydrate binding modules, *BMC Biotechnol.* 9 (2009) 92.
- [12] G.F. Vanzin, M. Madson, N.C. Carpita, N.V. Raikhel, K. Keegstra, W.-D. Reiter, The *mur2* mutant of *Arabidopsis thaliana* lacks fucosylated xyloglucan because of a lesion in fucosyltransferase AtFUT1, *Proc. Natl. Acad. Sci. U. S. A.* 99 (2002) 3340–3345.
- [13] D.M. VeytsmanCavalier, O. Lerouxel, L. Neumetzler, K. Yamauchi, A. Reinecke, G. Freshour, O.A. Zabotina, M.G. Hahn, I. Burgert, M. Pauly, N.V. Raikhel, K. Keegstra, Disrupting two *Arabidopsis thaliana* xylosyltransferase genes results in plants deficient in xyloglucan, a major primary cell wall component, *Plant Cell* 20 (2008) 1519–1537.
- [14] C. Xiao, T. Zhang, Y. Zheng, D.J. Cosgrove, C.T. Anderson, Xyloglucan deficiency disrupts microtubule stability and cellulose biosynthesis in *Arabidopsis*, altering cell growth and morphogenesis, *Plant Physiol. Biochem.* 170 (2016) 234–249.
- [15] O.A. Zabotina, W.T. van de Ven, G. Freshour, G. Drakakaki, D. Cavalier, G. Mouille, M.G. Hahn, K. Keegstra, N.V. Raikhel, *Arabidopsis XXT5* gene encodes a putative alpha-1,6-xylosyltransferase that is involved in xyloglucan biosynthesis, *Plant J.* 56 (2008) 101–115.
- [16] Y.B. Park, D.J. Cosgrove, Changes in cell wall biomechanical properties in the xyloglucan-deficient *xtt1/xtt2* mutant of *Arabidopsis*, *Plant Physiol.* 158 (2012) 465–475.
- [17] K. KAM1CTTamura, T. Shimada, M. Kondo, M. Nishimura, I. Hara-Nishimura, KATAMARI1/MURUS3 Is a novel Golgi membrane protein that is required for endomembrane organization in *Arabidopsis*, *Plant Cell* 17 (2005) 1764–1776.
- [18] W.D. Reiter, C. Chapple, C.R. Somerville, Mutants of *Arabidopsis thaliana* with altered cell wall polysaccharide composition, *Plant J.* 12 (1997) 335–345.
- [19] Y. Kong, M.J. Peña, L. Renna, U. Avci, S. Pattathil, S.T. Tuomivaara, X. Li, W.-D. Reiter, F. Brandizzi, M.G. Hahn, A.G. Darvill, W.S. York, M.A. O'Neill, Galactose-Depleted xyloglucan is dysfunctional and leads to dwarfism in *Arabidopsis*, *Plant Physiol.* 167 (2015) 1296–1306.
- [20] Z.J. Gong, Y.Q. Wu, J. Miao, Y. Duan, Y.L. Jiang, T. Li, Global transcriptome analysis of orange wheat blossom midge, *Sitodiplosis mosellana* (Gehin) (Diptera: Cecidomyiidae) to identify candidate transcripts regulating diapause, *PLoS One* 8 (2013) e71564.
- [21] J.D. Tedman-Jones, R. Lei, F. Jay, G. Fabro, X. Li, W.D. Reiter, C. Brearley, J.D. Jones, Characterization of *Arabidopsis mur3* mutations that result in constitutive activation of defence in petioles, but not leaves, *Plant J.* 56 (2008) 691–703.
- [22] Y.B. Park, D.J. Cosgrove, A revised architecture of primary cell walls based on biomechanical changes induced by substrate-specific endoglycanases, *Plant Physiol.* 158 (2012) 1933–1943.
- [23] S. Wolf, K. Hematy, H. Hofte, Growth control and cell wall signaling in plants, *Annu. Rev. Plant Biol.* 63 (2012) 381–407.
- [24] K. H'maty, P.-E. Sado, A. Van Tuinen, S. Rochange, T. Desnos, S. Balzergue, S. Pelletier, J.-P. Renou, H. Hofte, A receptor-like kinase mediates the response of *Arabidopsis* cells to the inhibition of cellulose synthesis, *Curr. Biol.* 17 (2007) 922–931.
- [25] B.D. Kohorn, S.L. Kohorn, The cell wall-associated kinases WAKs, as pectin receptors, *Front. Plant Sci.* 3 (2012) 1–5.
- [26] S. Wolf, D. van der Does, F. Ladwig, C. Sticht, A. Kolbeck, A.K. Schurholz, S. Augustin, N. Keinath, T. Rausch, S. Greiner, K. Schumacher, K. Harter, C. Zipfel, H. Hofte, A receptor-like protein mediates the response to pectin modification by activating brassinosteroid signaling, *Proc. Natl. Acad. Sci. U. S. A.* 111 (2014) 15261–15266.
- [27] M.D. Abramoff, P.J. Magalhaes, S.J. Ram, Image processing with ImageJ, 11, Biophotonics International, 2004, pp. 36–42.
- [28] C. Trapnell, B.A. Williams, G. Pertea, A. Mortazavi, G. Kwan, M.J. van Baren, S.L. Salzberg, B.J. Wold, L. Pachter, Transcript assembly and quantification by RNA-Seq reveals unannotated transcripts and isoform switching during cell differentiation, *Nat. Biotechnol.* 28 (2010) 511–515.

- [29] S. Anders, HTSeq: Analysing high-throughput sequencing data with Python, URL <http://www-huber.embl.de/users/anders/HTSeq/doc/overview.html>. (2010).
- [30] A. Mortazavi, B.A. Williams, K. McCue, L. Schaeffer, B. Wold, Mapping and quantifying mammalian transcriptomes by RNA-Seq, *Nat. Methods* 5 (2008) 621–628.
- [31] M.-A. Dillies, A. Rau, J. Aubert, C. Hennequet-Antier, M. Jeanmougin, N. Servant, C. Keime, G. Marot, D. Castel, J. Estelle, A comprehensive evaluation of normalization methods for Illumina high-throughput RNA sequencing data analysis, *Brief. Bioinf.* 14 (2013) 671–683.
- [32] L. Wang, Z. Feng, X. Wang, X. Zhang, DEGseq: an R package for identifying differentially expressed genes from RNA-seq data, *Bioinformatics* 26 (2010) 136–138.
- [33] Y. Benjamini, Y. Hochberg, Controlling the false discovery rate: a practical and powerful approach to multiple testing, *J. R. Stat. Soc. Ser. B (Methodol.)* (1995) 289–300.
- [34] Z. Du, X. Zhou, Y. Ling, Z. Zhang, Z. Su, agriGO: a GO analysis toolkit for the agricultural community, *Nucl. Acids Res.* 38 (2010) 64–70.
- [35] C. Xie, X. Mao, J. Huang, Y. Ding, J. Wu, S. Dong, L. Kong, G. Gao, C.-Y. Li, L. Wei, KOBAS 2.0: a web server for annotation and identification of enriched pathways and diseases, *Nucl. Acids Res.* 39 (2011) 316–322.
- [36] O. Thimm, O. Blasing, Y. Gibon, A. Nagel, S. Meyer, P. Kruger, J. Selbig, L.A. Muller, S.Y. Rhee, M. Stitt, MAPMAN: a user-driven tool to display genomics data sets onto diagrams of metabolic pathways and other biological processes, *Plant J.* 37 (2004) 914–939.
- [37] N. Mitsuda, M. Ohme-Takagi, Functional analysis of transcription factors in *Arabidopsis*, *Plant Cell Physiol.* 50 (2009) 1232–1248.
- [38] B. Zhang, S. Horvath, A general framework for weighted gene co-expression network analysis, *Stat. Appl. Genet. Mol. Biol.* 4 (2005) 1544–6115.
- [39] R. Saito, M.E. Smoot, K. Ono, J. Ruscheinski, P.-L. Wang, S. Lotia, A.R. Pico, G.D. Bader, T. Ideker, A travel guide to Cytoscape plugins, *Nat. Methods* 9 (2012) 1069–1076.
- [40] S.J. Clough, A.F. Bent, Floral dip: a simplified method for Agrobacterium-mediated transformation of *Arabidopsis thaliana*, *Plant J.* 16 (1998) 735–743.
- [41] K.J. Livak, T.D. Schmittgen, Analysis of relative gene expression data using real-time quantitative PCR and the 2(-Delta Delta CT) method, *Methods* 25 (2001) 402–408.
- [42] Y.B. Park, D.J. Cosgrove, Xyloglucan and its interactions with other components of the growing cell wall, *Plant Cell Physiol.* 56 (2015) 180–194.
- [43] E. Jamet, D. Roujol, H. San-Clemente, M. Irshad, L. Soubigou-Taconnat, J.-P. Renou, R. Pont-Lezica, Cell wall biogenesis of *Arabidopsis thaliana* elongating cells: transcriptomics complements proteomics, *BMC Genomics* 10 (2009) 1–12.
- [44] P. Derbyshire, K. Findlay, M.C. McCann, K. Roberts, Cell elongation in *Arabidopsis* hypocotyls involves dynamic changes in cell wall thickness, *J. Exp. Bot.* 58 (2007) 2079–2089.
- [45] M. Irshad, H. Canut, G. Borderies, R. Pont-Lezica, E. Jamet, A new picture of cell wall protein dynamics in elongating cells of *Arabidopsis thaliana*: confirmed actors and newcomers, *BMC Plant Biol.* 8 (2008) 94–110.
- [46] W.D. Teale, I.A. Paponov, K. Palme, Auxin in action: signalling, transport and the control of plant growth and development, *Nat. Rev. Mol. Cell Biol.* 7 (2006) 847–859.
- [47] E.J. Chapman, M. Estelle, Mechanism of auxin-regulated gene expression in plants, *Ann. Rev. Genet.* 43 (2009) 265–285.
- [48] S. Wolf, J. Mravec, S. Greiner, G. Mouille, H. Hofte, Plant cell wall homeostasis is mediated by brassinosteroid feedback signaling, *Curr. Biol.* 22 (2012) 1732–1737.
- [49] Q. Tian, J. Reed, Control of auxin-regulated root development by the *Arabidopsis thaliana SHY2/IAA3* gene, *Development* 126 (1999) 711–721.
- [50] H. Leyser, F.B. Pickett, S. Dharmasiri, M. Estelle, Mutations in the AXR3 gene of *Arabidopsis* result in altered auxin response including ectopic expression from the SAUR-AC1 promoter, *Plant J.* 10 (1996) 403–413.
- [51] B.C. Kim, M.S. Soh, B.J. Kang, M. Furuya, H.G. Nam, Two dominant photomorphogenic mutations of *Arabidopsis thaliana* identified as suppressor mutations of *hy2*, *Plant J.* 9 (1996) 441–456.
- [52] P.J. Overvoorde, Y. Okushima, J.M. Alonso, A. Chan, C. Chang, J.R. Ecker, B. Hughes, A. Liu, C. Onodera, H. Quach, Functional genomic analysis of the *AUXIN/INDOLE-3-ACETIC ACID* gene family members in *Arabidopsis thaliana*, *Plant Cell* 17 (2005) 3282–3300.
- [53] S.D. Clouse, J.M. Sasse, BRASSINOSTEROIDS: essential regulators of plant growth and development, *Annu. Rev. Plant Physiol. Plant Mol. Biol.* 49 (1998) 427–451.
- [54] Y. Sun, X.Y. Fan, D.M. Cao, W. Tang, K. He, J.Y. Zhu, J.X. He, M.Y. Bai, S. Zhu, E. Oh, S. Patil, T.W. Kim, H. Ji, W.H. Wong, S.Y. Rhee, Z.Y. Wang, Integration of brassinosteroid signal transduction with the transcription network for plant growth regulation in *Arabidopsis*, *Dev. Cell.* 19 (2010) 765–777.
- [55] G. Vert, J.L. Nemhauser, N. Geldner, F. Hong, J. Chory, Molecular mechanisms of steroid hormone signaling in plants, *Annu. Rev. Cell Dev. Biol.* 21 (2005) 177–201.
- [56] T. Takahashi, A. Gasch, N. Nishizawa, N.-H. Chua, The *DIMUNTO* gene of *Arabidopsis* is involved in regulating cell elongation, *Genes Dev.* 9 (1995) 97–107.
- [57] J. Chory, P. Nagpal, C.A. Peto, Phenotypic and genetic analysis of *det2*, a new mutant that affects light-regulated seedling development in *Arabidopsis*, *Plant Cell* 3 (1991) 445–459.
- [58] K.A. Feldmann, M.D. Marks, M.L. Christianson, R.S. Quatrano, A dwarf mutant of *Arabidopsis* generated by T-DNA insertion mutagenesis, *Science* 243 (1989) 1351–1354.
- [59] A. Kauschmann, A. Jessop, C. Koncz, M. Szekeres, L. Willmitzer, T. Altmann, Genetic evidence for an essential role of brassinosteroids in plant development, *Plant J.* 9 (1996) 701–713.
- [60] K. Hematy, H. Hofte, Novel receptor kinases involved in growth regulation, *Curr. Opin. Plant Biol.* 11 (2008) 321–328.
- [61] B.D. Kohorn, WAKs; cell wall associated kinases, *Curr. Opin. Cell Biol.* 13 (2001) 529–533.
- [62] P.M. Ray, P.B. Green, R. Cleland, Role of Turgor in Plant Cell Growth, 1972.
- [63] G. Guerriero, J.-F. Hausman, G. Cai, No stress! Relax! Mechanisms governing growth and shape in plant cells, *Int. J. Mol. Sci.* 15 (2014) 5094–5114.
- [64] D.J. Cosgrove, Growth of the plant cell wall, *Nat. Rev. Mol. Cell Biol.* 6 (2005) 850–861.
- [65] U.G. Hacke, J. Laur, Aquaporins: channels for the molecule of life, *Encyclopedia Life Sci.* (2016) 1–6.
- [66] R. Aharon, Y. Shahak, S. Wininger, R. Bendov, Y. Kapulnik, G. Galili, Overexpression of a plasma membrane aquaporin in transgenic tobacco improves plant vigor under favorable growth conditions but not under drought or salt stress, *Plant Cell* 15 (2003) 439–447.
- [67] B. Péret, G. Li, J. Zhao, L.R. Band, U. Voß, O. Postaire, D.-T. Luu, O. Da Ines, I. Casimiro, M. Lucas, Auxin regulates aquaporin function to facilitate lateral root emergence, *Nat. Cell Biol.* 14 (2012) 991–998.
- [68] D. Bellincampi, F. Cervone, V. Lionetti, Plant cell wall dynamics and wall-related susceptibility in plant-pathogen interactions, *Front. Plant Sci.* 5 (2014) 1–8.
- [69] V. Lionetti, F. Cervone, D. Bellincampi, Methyl esterification of pectin plays a role during plant-pathogen interactions and affects plant resistance to diseases, *J. Plant Physiol.* 169 (2012) 1623–1630.
- [70] S. Ferrari, D.V. Savatin, F. Sicilia, G. Gramigna, F. Cervone, G.D. Lorenzo, Oligogalacturonides: plant damage-associated molecular patterns and regulators of growth and development, *Front. Plant Sci.* 4 (2013) 49.
- [71] G. Pogorelko, V. Lionetti, D. Bellincampi, O. Zabotina, Cell wall integrity: targeted post-synthetic modifications to reveal its role in plant growth and defense against pathogens, *Plant Signal. Behav.* 8 (2013) 1–8.
- [72] G. Bethke, A. Thao, G. Xiong, B. Li, N.E. Soltis, N. Hatsugai, R.A. Hillmer, F. Katagiri, D.J. Kliebenstein, M. Pauly, J. Glazebrook, Pectin biosynthesis is critical for cell wall integrity and immunity in *Arabidopsis thaliana*, *Plant Cell* 28 (2016) 537–556.
- [73] V. Lionetti, F. Cervone, D. Bellincampi, Methyl esterification of pectin plays a role during plant-pathogen interactions and affects plant resistance to diseases, *J. Plant Physiol.* 169 (2012) 1623–1630.
- [74] V. Lionetti, A. Raola, L. Camardella, A. Giovane, N. Obel, M. Pauly, F. Favaron, F. Cervone, D. Bellincampi, Overexpression of pectin methylesterase inhibitors in *Arabidopsis* restricts fungal infection by *Botrytis cinerea*, *Plant Physiol.* 143 (2007) 1871–1880.
- [75] C. Volpi, M. Janni, V. Lionetti, D. Bellincampi, F. Favaron, R. D'ovidio, The ectopic expression of a pectin methyl esterase inhibitor increases pectin methyl esterification and limits fungal diseases in wheat, *Mol. Plant Microbe Interact.* 24 (2011) 1012–1019.